


# Novel strategy of ovarian cancer implantation: Pre-invasive growth of fibrin-anchored cells with neovascularization

Ayumi Matsuoka<sup>1</sup> | Yasunari Mizumoto<sup>1</sup>  | Masanori Ono<sup>1</sup> | Kyosuke Kagami<sup>1</sup> | Takeshi Obata<sup>1</sup> | Junpei Terakawa<sup>2</sup> | Yoshiko Maida<sup>3</sup> | Mitsuhiro Nakamura<sup>1</sup> | Takiko Daikoku<sup>2</sup> | Hiroshi Fujiwara<sup>1</sup>

<sup>1</sup>Department of Obstetrics and Gynecology, Graduate School of Medical Sciences, Kanazawa University, Kanazawa, Japan

<sup>2</sup>Institute for Experimental Animals, Advanced Science Research Center, Kanazawa University, Kanazawa, Japan

<sup>3</sup>Department of Nursing, College of Medical, Pharmaceutical, and Health Sciences, Kanazawa University, Kanazawa, Japan

## Correspondence

Yasunari Mizumoto, Department of Obstetrics and Gynecology, Kanazawa University Graduate School of Medical Science, 13-1, Takaramachi, Kanazawa, Ishikawa 920-8641, Japan.  
Email: yas1025@med.kanazawa-u.ac.jp

## Funding information

Grants-in-Aid for Scientific Research, Grant/Award Number: 17H04337 and 18K16762

## Abstract

Although direct adhesion of cancer cells to the mesothelial cell layer is considered to be a key step for peritoneal invasion of ovarian cancer cell masses (OCM), we recently identified a different strategy for the peritoneal invasion of OCM. In 6 out of 20 cases of ovarian carcinoma, extraperitoneal growth of the OCM was observed along with the neovascularization of feeding vessels, which connect the intraperitoneal host stroma and extraperitoneal lesions through the intact mesothelial cell layer. As an early step, the OCMs anchor in the extraperitoneal fibrin networks and then induce the migration of CD34-positive and vascular endothelial growth factor A (VEGF-A)-positive endothelial cells, constructing extraperitoneal vascular networks around the OCM. During the extraperitoneal growth of OCM, podoplanin-positive and  $\alpha$  smooth muscle actin ( $\alpha$ SMA)-positive cancer-associated fibroblasts (CAF) appears. In more advanced lesions, the boundary line of mesothelial cells disappears around the insertion areas of feeding vessels and then extraperitoneal and intraperitoneal stroma are integrated, enabling the OCM to invade the host stroma, being associated with CAF. In addition, tissue factors (TF) are strongly detected around these peritoneal implantation sites and their levels in ascites were higher than that in blood. These findings demonstrate the presence of neovascularization around fibrin net-anchored OCMs on the outer side of the intact peritoneal surface, suggesting a novel strategy for peritoneal invasion of ovarian cancer and TF-targeted intraperitoneal anti-cancer treatment. We observed and propose a novel strategy for peritoneal implantation of ovarian cancer. The strategy includes the preinvasive growth of fibrin-anchored cancer cells along with neovascularization on the outer side of the intact peritoneal surface.

## KEYWORDS

extraperitoneal neovascularization, mesothelial barrier, ovarian cancer cell mass, peritoneal invasion, tissue factor

**Abbreviations:**  $\alpha$ SMA,  $\alpha$  smooth muscle actin; CAF, cancer-associated fibroblasts; CXCL12, C-X-C motif chemokine ligand 12; EMT, epithelial-to-mesenchymal transition; MET, mesenchymal-to-epithelial transition; OCM, ovarian cancer cell mass; SDF-1, stromal cell-derived factor-1; TF, tissue factor; VEGF, vascular endothelial growth factor.

This is an open access article under the terms of the Creative Commons Attribution-NonCommercial License, which permits use, distribution and reproduction in any medium, provided the original work is properly cited and is not used for commercial purposes.

© 2019 The Authors. *Cancer Science* published by John Wiley & Sons Australia, Ltd on behalf of Japanese Cancer Association

## 1 | INTRODUCTION

Peritoneal dissemination is one of the main routes of metastasis in ovarian cancer. More than 75% of patients with ovarian cancer are diagnosed with metastases at advanced stages throughout the pelvic and peritoneal cavities.<sup>1-3</sup> Intraperitoneal dissemination of epithelial ovarian cancer cells is considered to be initiated by the shedding of tumor cells from the primary site into peritoneal fluids. Then, these tumor cells form free-floating multicellular masses, an ovarian cancer cell masses (OCM), and serve as a vehicle for widespread dissemination in the peritoneal cavity.<sup>4</sup> OCMs effused from cystic fluid in ovarian cancer were also reported to contribute to intraperitoneal dissemination.<sup>5,6</sup> During these processes, the process of disconnection of cell-to-cell interactions has been shown to play a significant role in cells leaving the primary site and metastasizing to a distant site.<sup>4</sup>

Currently, it is widely accepted that the development of peritoneal metastasis is a multistep process, as follows: (a) detachment of cancer cells from the primary tumor; (b) survival in the microenvironment of the abdominal cavity as single cells or OCM; (c) attachment of free tumor cells to peritoneal mesothelial cells; (d) invasion beyond the mesothelial layer; and (e) tumor growth with the onset of angiogenesis.<sup>7,8</sup> However, it remains unclear how free-floating OCM can invade the peritoneal stroma beyond the mesothelial cell layer. To explain this process, EMT and MET, which are important mechanisms for cell attachment, disaggregation, and migration, regulating the invasion and metastasis of cancer, were also proposed to be involved in these processes.<sup>7-10</sup>

In contrast with this concept, preparing a specific paraffin-embedded block of peritoneal lesions, we recently observed unique histological features in which OCMs grow along with neovascularization on the outer side of the intact peritoneal surface (extraperitoneal space) in the absence of direct attachment to the peritoneal epithelial cells, and then invade the peritoneal stroma (intraperitoneal space). Consequently, here we propose a novel pathway that can achieve successful peritoneal implantation of OCM.

## 2 | MATERIALS AND METHODS

### 2.1 | Immunohistochemistry

Twenty patients with ovarian carcinoma and with peritoneal dissemination, who underwent primary debulking surgery or exploratory laparotomy at Kanazawa University Hospital, Japan, were recruited into this study. The study was approved by the ethical committee at Kanazawa University and preoperative informed consent was obtained from the patients. Peritoneal specimens were fixed in 10% formalin under widely spreading conditions and then cut to 5 mm in width, placed vertically in cassettes and embedded in paraffin, and sliced into 3- $\mu$ m sections. At sites where the "extraperitoneal growth of OCM" were observed, 10 serial sections were additionally made for further investigation. The immunohistochemical staining method was performed as reported previously.<sup>11</sup> Briefly, heat-induced epitope retrieval was performed by boiling the deparaffinized tissue sections in .01 mol/L citrate buffer. After

blocking endogenous peroxidase activity, the slides were incubated with mouse monoclonal antibodies against TF (clone: 2K1, Abcam, Cambridge, UK), fibrinogen alpha chain (clone: UC45, Abcam, Cambridge, UK), CD34 (clone: QBEnd-10, Dako, Carpinteria, USA), podoplanin (clone: D2-40, Dako, Carpinteria, USA),  $\alpha$ SMA (clone: 1A4, Dako, Carpinteria, USA), VEGF-A (clone: VG1, Dako, Carpinteria, USA), E-cadherin (clone: G-10, Santa Cruz Biotechnology, Dallas, USA), rabbit monoclonal antibodies against CD31 (clone: EPR3094, Abcam, Cambridge, UK), and rabbit polyclonal antibodies against SDF-1/CXCL12 (Abcam, Cambridge, UK) at 4°C overnight in a humidified box. After washing, the sections were incubated for 30 min with biotin-labeled horse anti-mouse or goat anti-rabbit immunoglobulin G (IgG) at room temperature, and then treated with the avidin-biotin complex (VECTASTAIN ABC kit; Vector Laboratories, Burlingame, USA). Sites of peroxidase activity were visualized with diaminobenzidine (Liquid DAB+ Substrate Chromogen System; Dako, Carpinteria, USA). After counterstaining with hematoxylin, specimens were dehydrated and mounted.

### 2.2 | Enzyme-linked immunosorbent assay

Enzyme-linked immunosorbent assay (ELISA) was performed to confirm the presence of TF in ascitic fluids and blood of patients with ovarian cancer. TF was measured by ELISA using a commercial kit (Quantikine Human Coagulation Factor III/Tissue Factor Immunoassay, R&D Systems, Minneapolis, USA) according to the manufacturer's instructions. All samples were measured in duplicate by a single operator using assay kits from the same lot.

### 2.3 | RNA extraction and reverse transcription polymerase chain reaction

RNA was extracted from frozen tumor samples to detect TF levels using an RNeasy Mini Kit (Qiagen, Helden, Germany). After DNase treatment (Ambion Diagnostics Inc. Austin, USA), 1  $\mu$ g of total RNA was reverse transcribed with SuperScript II (Invitrogen, Carlsbad, USA), according to the manufacturer's instructions. Primer sequences were: 5'-GCCAGGAGAAAGGGGAAAT-3' and 5'-CAGTGCAATATAGCATTTCAGTAGC-3' for TF, 5'-GCACCGTCAAGGCTGAGAAC-3' and 5'-TGGTGAAGACGCCAGTGGA-3' for GAPDH. PCR was performed for 50 cycles at 95°C for 30 s, 60°C for 30 s, and 72°C for 30 s, in accordance with a previous report.<sup>12</sup> After amplification, the resulting PCR products were purified with a MinElute Gel Extraction Kit (Qiagen). The purified PCR products were sequenced and detected using a DNA sequencer (3730xl DNA Analyzer; Thermo Fisher Scientific).

### 2.4 | Statistical methods

Statistical analysis was performed using the Statistical Package for the Social Sciences software, version 23 for Windows (SPSS). Continuous variables were compared using the Mann-Whitney *U* test and Wilcoxon signed-rank test, and are presented as the median and interquartile range.

### 3 | RESULTS

#### 3.1 | New strategy for peritoneal implantation: neovascularization around fibrin net-anchored OCM on the outer side of the intact peritoneal surface

Twenty patients with ovarian carcinoma were recruited in this study. All showed deep invasion of cancer cells in the peritoneal stromal tissues. Eleven had high-grade serous carcinoma, and the remaining patients had mucinous carcinoma (n = 1), low-grade serous carcinoma (n = 2), poorly differentiated adenocarcinoma (n = 3), adenocarcinoma (n = 1), and clear cell carcinoma (n = 2). Among 13 patients with serous carcinoma, in 6 (case #1-5,12, Table 1) cases, 4 to 7 slides per case were evaluable for peritoneal implantation. Two to 6 sites of "extraperitoneal growth of OCM," in which blood flow was supplied through the feeding vessel from the host stroma lined with intact mesothelial, were observed near the small invasive lesions in each cases, whereas no invasion was observed at the site in 10 serial sections. In 7 cases, only 1 or 2 slides per case were available for evaluation and only gross invasive tumors, without small metastatic regions or "extraperitoneal growth of OCM," were observed. The extraperitoneal growth of the OCMs was enveloped by fibrous structures and accompanied with straight or tortuous vascular

connections between the intraperitoneal host stroma and extraperitoneal lesions similar to in-air refueling of an airship, showing fine stromal tissues without cancer cell invasion. (airship-refueling sign: Figure 1A,B).

Among these 6 patients, 1 patient (case #1) showed various stages of peritoneal implantation and invasion of OCM. In the peritoneal lesions, OCMs (Figure 1C-O) were shown to be enveloped by thin fibrous structures, partially contacting the fibrous net without destroying or attaching to intact peritoneal epithelium (Figure 1C-O). Immunoreactive fibrinogen was detected on these fibrous tissues (Figure 1G), indicating that this structure was composed of fibrin networks, being consistent with previous reports.<sup>13,14</sup> We also observed the presence of TF in the fibrous tissues (Figure 1H), this presence can initiate plasma coagulation protease cascades including the transformation of fibrin from fibrinogen. Importantly, migration of fibroblasts (Figure 1D,F) was observed along the fibrin-net structures, whereas mesothelial cells highly expressed podoplanin, a marker of mesothelial cells, showing the intact peritoneal line as a peritoneal barrier (Figure 1E,F).

In addition, CD34-positive endothelial cells migrated alongside these fibrin-net structures (Figure 1I,J). These fibroblastic cells expressed VEGF-A highly (Figure 1K,L). Notably, in the adjacent lesions, fine vascular networks containing red blood cells had been already

**TABLE 1** Clinical and pathological data on 20 patients assessed by immunohistochemical study

Case	Age	Histology	Stage	TF in blood	TF in ascites (pg/mL)	Airship findings	TF
1	40	HGSOC	IIIC	-	-	+	++
2	70	HGSOC	IVA	12.89	71.37	+	+
3	42	HGSOC	IIIC	-	46.48	+	+
4	49	HGSOC	IIIC	-	-	+	++
5	53	HGSOC	IIIC	8.54	208.98 → 5.39*	+	+
6	73	HGSOC	IIIC	-	21.59	-	+
7	64	HGSOC	IIIC	-	182.89	-	++
8	63	HGSOC	IIIC	5.72	383.76	-	+
9	52	HGSOC	IIIC	-	48.65	-	+
10	72	HGSOC	IIIB	21.91	680.61	-	++
11	66	HGSOC	IIIC	8.65*	365.28 → 183.76*	-	++
12	63	Low-grade serous	IIIB	-	-	+	++
13	68	Low-grade serous	IIIA	-	-	-	+
14	48	Mucinous	IIIB	26.26	365.72	-	+
15	42	Poor differentiation	IIIB	6.70*	47.02*	-	++
16	55	Poor differentiation	IIIC	13.98	-	-	+
17	68	Poor differentiation	IVB	-	-	-	++
18	65	Clear	IIIC	-	686.04	-	++
19	59	Clear	IIIC	-	-	-	++
20	73	Adenocarcinoma	IVB	-	70.07	-	+

Abbreviations: HGSOC, high-grade serous ovarian carcinoma; TF, immunohistochemical expression of TF; + moderately positive; ++ strongly positive; \*, post chemotherapy.

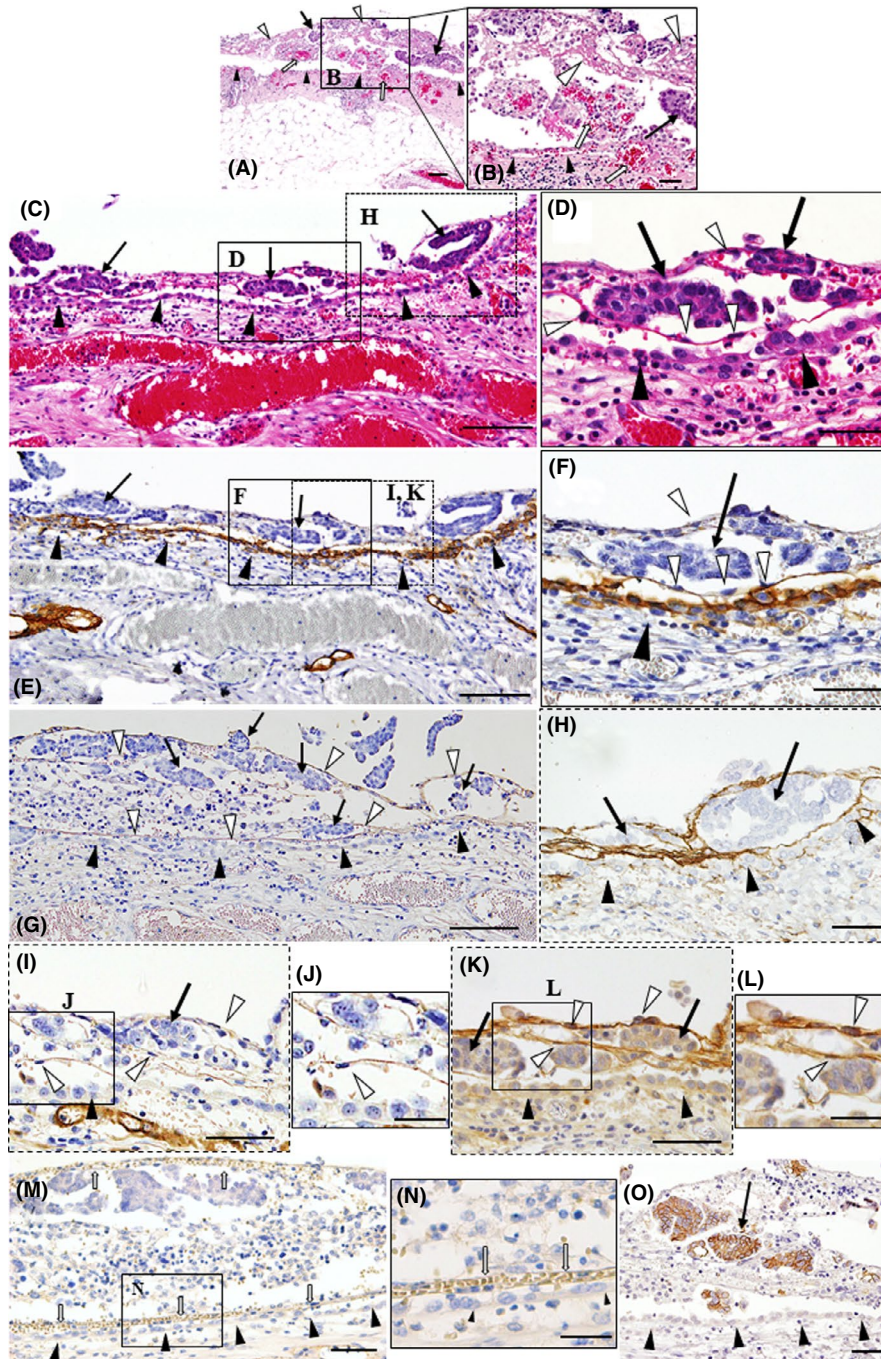


**FIGURE 1** Ovarian cancer cell masses (OCMs) on the outer side of the intact peritoneal surface in patients with high-grade serous carcinoma (cases #1 and 2). Staining of hematoxylin and eosin (A–D), podoplanin (E, F), fibrinogen (G), transfer factor (TF) (H), CD34 (I, J), vascular endothelial growth factor A (VEGF-A) (K, L), CD31 (M, N), and E-cadherin (O). Case #2 (A, B), case #1 (C–O). A, B, Extraperitoneal OCMs (black arrows) received straight or tortuous feeding vessels (white arrows) from the noninvaded host stroma that was lined by intact mesothelial cells (black arrowheads). White arrowheads in (A) and (B) show fibrous structures around OCMs. C–O, numerous OCM (black arrows) were enveloped by the thin fibrous structures without destroying or attaching to intact peritoneal epithelium (black arrowheads). C–F, migration of fibroblasts was observed along the fibrin-net structures (white arrowheads). Podoplanin was highly expressed on intact mesothelial cells (black arrowheads). G, Adjacent sites of (C, E) immunoreactive fibrinogen were detected on the thin fibrous tissues (white arrowheads). H, TF was detected on these fibrous tissues. I–L, CD34 and VEGF-A expression was detected on the migrating cells (white arrowheads) alongside the fibrin-net structures. M, N, Adjacent sites of (G), fine vascular networks (white arrows) containing red blood cells were constructed by CD31-positive endothelial cells on the outside of the intact mesothelial cell layer (black arrowheads). O, Adjacent sites of (G) E-cadherin, which designate epithelioid phenotype, were dominant in fibrin-anchored OCMs on the outer side of the intact peritoneal surface. Bars show 100  $\mu\text{m}$  (A, C, E, G), and 50  $\mu\text{m}$  (B, D, F, H, I, K, M, O) and 25  $\mu\text{m}$  (J, L, N)

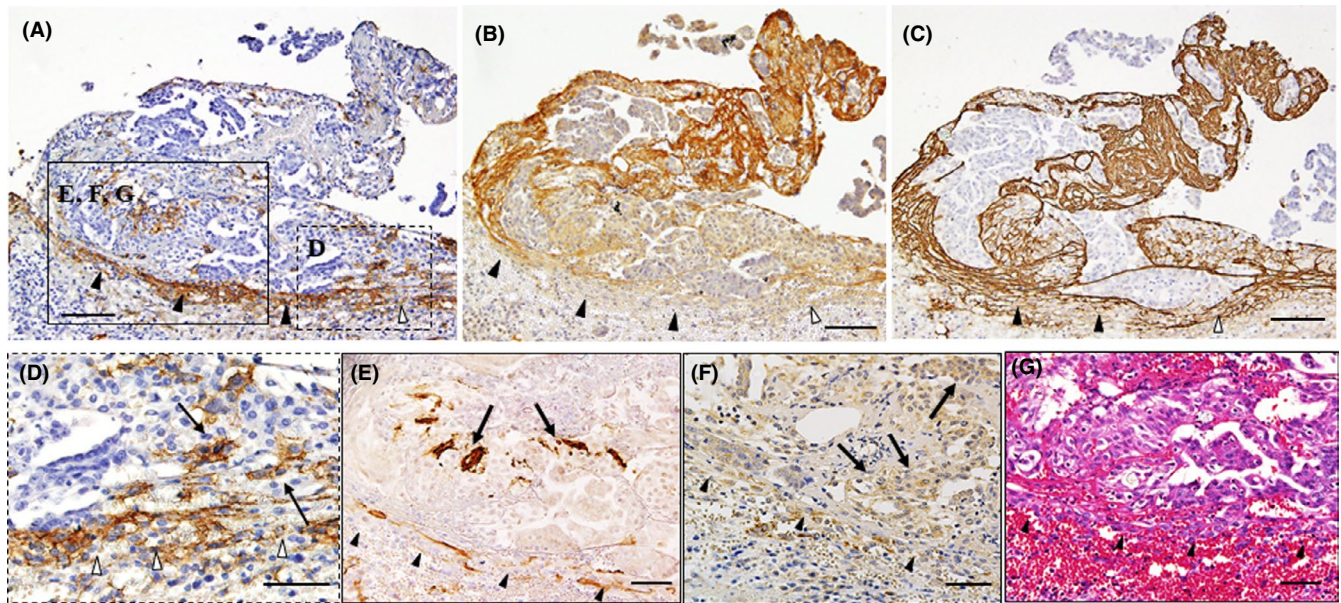


**FIGURE 2** Extraperitoneal neovascularization around ovarian cell mass (OCM) in case #1. Staining of podoplanin (A, D), vascular endothelial growth factor (VEGF-A) (B), transfer factor (TF) (C),  $\alpha$  smooth muscle actin ( $\alpha$ SMA) (E), stromal cell-derived factor-1/C-X-C motif chemokine ligand 12 (SDF-1/CXCL12) (F), and hematoxylin and eosin (G). A-C, At a more advanced site than Figure 1. B, Expression of VEGF-A was shown on stromal tissues around OCMs. C, TF was also highly expressed around OCM. D, E, Podoplanin-positive and  $\alpha$ SMA-positive CAF (black arrows) were observed among OCM. F, OCMs and stromal cells expressed SDF-1/CXCL12 (black arrows). G, Vascular dilatation was evident in the stromal tissues around the OCM and abundant extravasation of red blood cells was observed beneath mesothelial cells. A, D, G, Around the area where numerous vessels traverse beyond the boundary, the line of podoplanin-positive mesothelial cells was disrupted (intact peritoneal epithelium: black arrowheads, disrupted mesothelial cell layer: white arrowheads). Bars show 100  $\mu$ m (A, B, C), 50  $\mu$ m (D, E, F, G)

constructed by CD31-positive or CD34-positive endothelial cells on the outside of the intact mesothelial cell layer, providing blood supply to the OCMs from the host peritoneal stroma (Figure 1M,N).

At more advanced sites (Figure 2A-C), CAF, which were defined as podoplanin-positive or  $\alpha$ SMA-positive spindle-shaped cells, became distinct among OCMs (Figure 2D,E), and these OCMs expressed SDF-1/CXCL12 (Figure 2F). In addition, vascular dilatation was evident in the stromal tissues around the OCMs (Figure 2G). Consistent with the above findings, VEGF-A was strongly deposited on the stromal tissues around the OCMs (Figure 2B). Importantly, abundant extravasation of red blood cells was observed beneath mesothelial cells (Figure 2G). Around the area where numerous vessels traversed beyond the boundary, the line of podoplanin-positive mesothelial cells was disrupted (Figure 2A,D). These findings show the presence of active inflammation and a tissue remodeling reaction at the interface between the OCM and host stromal tissues, and suggest that the mesothelial boundary line may initially disappear around the insertion sites of feeding vessels under the influence of the OCM. High-level expression of TF was also observed in these areas (Figure 2C).

At further advanced sites (Figure 3), the boundary line of mesothelial cells widely disappeared and both peritoneal and OCM-surrounding stromal tissues were completely integrated together (Figure 3A-C); this action can be confirmed by the presence of freely communicating CAF beyond the boundary (Figure 3B). In some regions, these integrated areas were fused together and invading OCMs were

predominantly observed around the feeding vessels (Figure 3D-F). This situation enables the OCM to invade the peritoneal stroma, being associated with CAF (Figure 3G-I). The high expression of TF was also observed around the OCM (Figure 3C,I).

### 3.2 | Identification of TF in ascitic fluid and peritoneal metastatic lesions

As TF was strongly expressed around the peritoneal dissemination site of cancer cells, we measured plasma and ascitic TF levels ( $n = 25$  and  $n = 20$ , respectively) in patients with ovarian cancer ( $n = 33$ ). The median value of ascitic TF was significantly higher than that of plasma TF (Figure 4A). In 12 patients, we could obtain both plasma and ascitic samples and compare these, confirming that the TF level in ascites was higher than that in blood (Figure 4B). In 2 of these, the ascitic levels of TF decreased in accordance with the time course of chemotherapy (Table 1). In case #12, mRNA expression of TF was confirmed by RT-PCR both in primary and peritoneal metastatic regions (Table 1 and Figure 4C).

## 4 | DISCUSSION

In this study, we observed unique histological features of peritoneal invasion of OCMs in 6 of 13 patients with serous carcinoma, showing

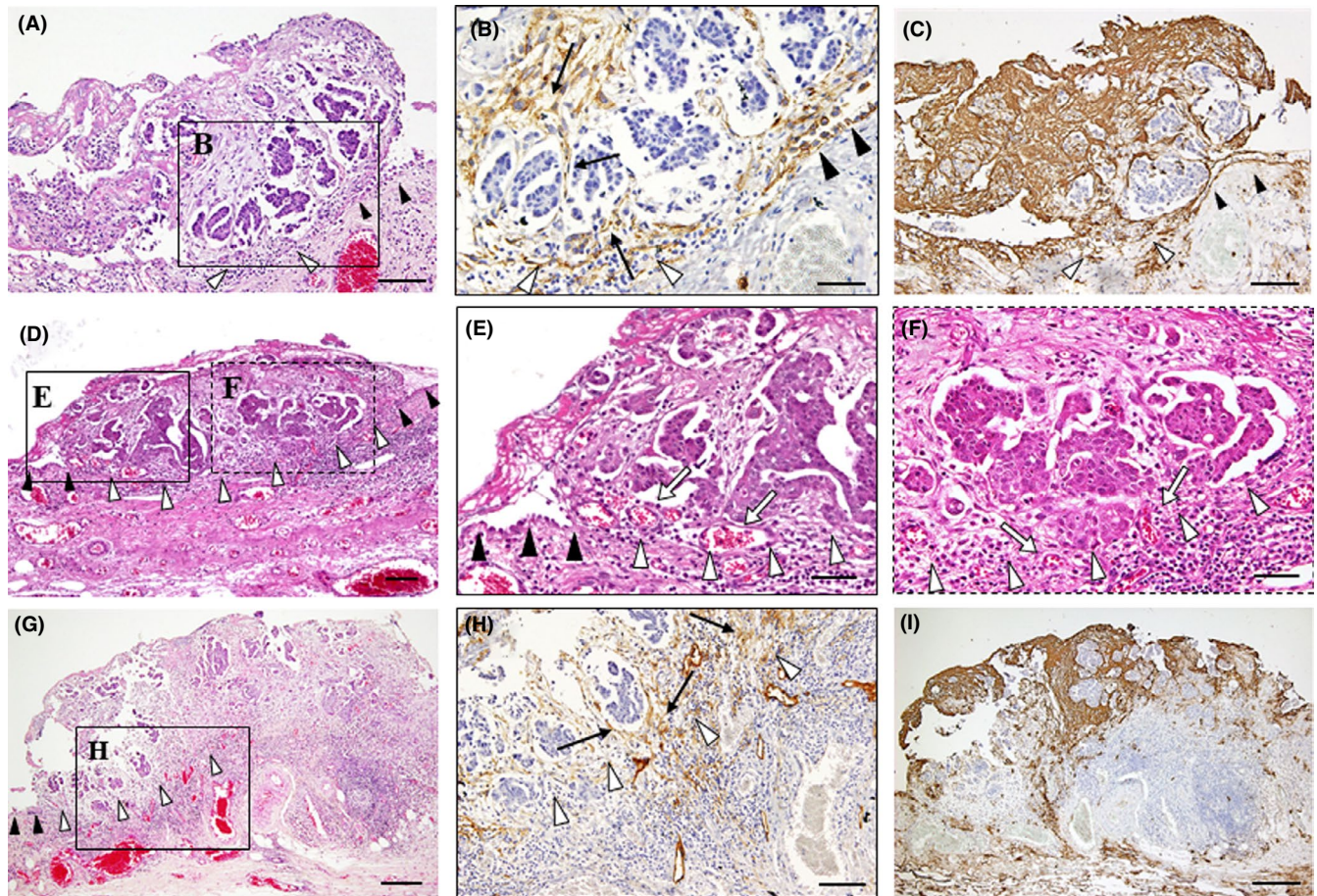


**FIGURE 3** Invasion of ovarian cell mass (OCM) toward peritoneal stroma in case #1. Staining of hematoxylin and eosin (A, D–G), podoplanin (B, H), and transfer factor (TF) (C, I). A–C, At a more advanced site than Figure 2. The boundary line of mesothelial cells widely disappeared (white arrowheads) and both peritoneal and OCM-surrounding stromal tissues were completely integrated together (black arrows). D–F, These integrated areas were fused together and invading OCM were predominantly observed around the feeding vessels (white arrows). G, H, OCMs invade the peritoneal stroma, being associated with CAF (black arrows). I, TF was highly expressed around OCM. Black arrowheads show intact mesothelial cell layer and white arrowheads show disrupted mesothelial cells. Bars show 200  $\mu\text{m}$  (G, I), 100  $\mu\text{m}$  (A, C, D, H), and 50  $\mu\text{m}$  (B, E, F)

extraperitoneal growth without attachment to intact mesothelial cells with blood supply from the intraperitoneal host stroma. As the structure of the tortuous vascular connection between intraperitoneal host stroma and extraperitoneal lesions resembled in-air refueling of an airship, we named it the “airship-refueling sign.” In all 6 cases, deep peritoneal invasion was observed, suggesting the presence of a new alternative pathway to achieve successful peritoneal implantation. To clarify the mechanisms for this unique strategy of peritoneal invasion, we performed an additional immunohistochemical study and observed several findings.

Based on these results, we suggest the following sequential steps: (i) OCMs cause an inflammatory reaction on the peritoneal stroma, inducing the leakage of fibrinogen (step I, Figure 5A); (ii) OCM are anchored in fine fibrin networks and then surrounded by the networks without adhering to the peritoneal epithelium, inducing migration of fibroblasts and endothelial cells from the host's tissues toward the fibrin networks (step II, Figure 5B); (iii) fibrin networks around the OCM become mature stromal tissues, developing

vascular networks, growing OCMs, differentiating CAF, inducing inflammation around vessel insertion sites, and extending the opening of the intact mesothelial cell layer (step III, Figure 5C); and (iv) the boundary layer of mesothelial cells disappears and both intraperitoneal host stromal tissues and extraperitoneal OCM-surrounding stromal tissues are integrated together; this process enables the OCM to invade the host stroma, being accompanied by CAF (step IV, Figure 5D).

To explain the above steps, we further suggested the following mechanisms. As the 1st step, OCMs induce leakage of fibrinogen on the surface of the peritoneal wall. Although we have no definite evidence for this step, previous studies have demonstrated that tumor cells in ascites can induce superficial microvascular congestion and hyperpermeability in the underlying stroma of the peritoneum, and fibrin deposition on the surface of peritoneal epithelial cells.<sup>13,14</sup> Being consistent with these reports, we observed abundant dilated vessels with the accumulation of VEGF-A in the stroma under the intact mesothelial cell layer that faces the OCM.

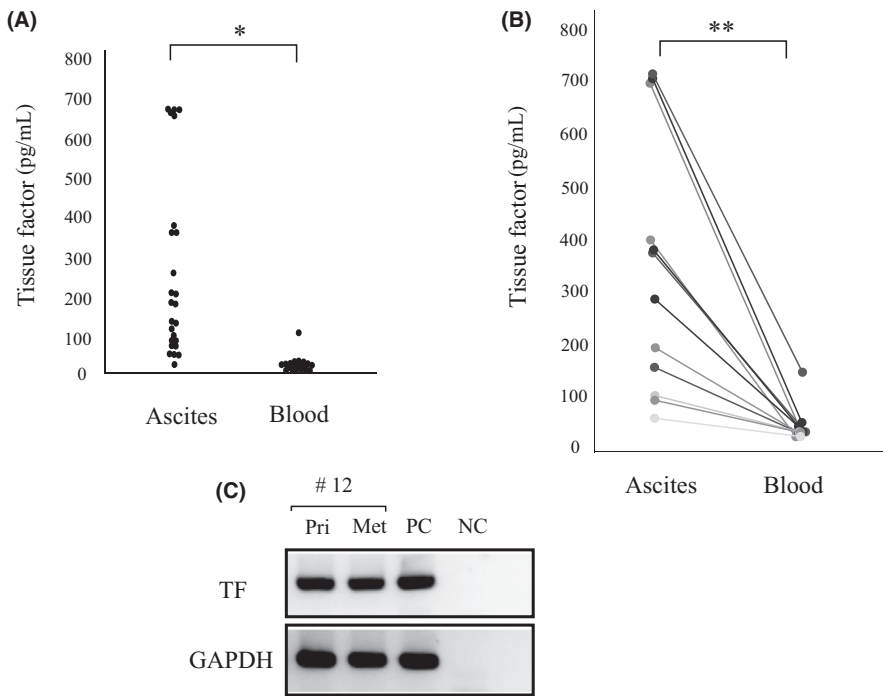


**FIGURE 4** The ascitic and plasma levels of transfer factor (TF) in patients with ovarian cancer. The plasma and ascitic TF levels ( $n = 25$  and  $n = 20$ , respectively) were measured in patients (total  $n = 33$ ) with ovarian cancer. A, The median value of ascitic TF was significantly higher than that of plasma TF. B, In 12 cases, we could obtain both plasma and ascitic samples. It was also confirmed that the TF level in ascites was higher than that in blood. C, RT-PCR was performed to confirm the presence of TF in the tissue of ovarian cancer (case #11). mRNA expression of TF was confirmed both in primary and peritoneal metastatic regions. Met, peritoneal metastasis; NC, negative control; PC, positive control (ovarian cancer cell line; SKOV3); Pri, primary lesion. \* $P < .001$ . \*\* $P = .001$

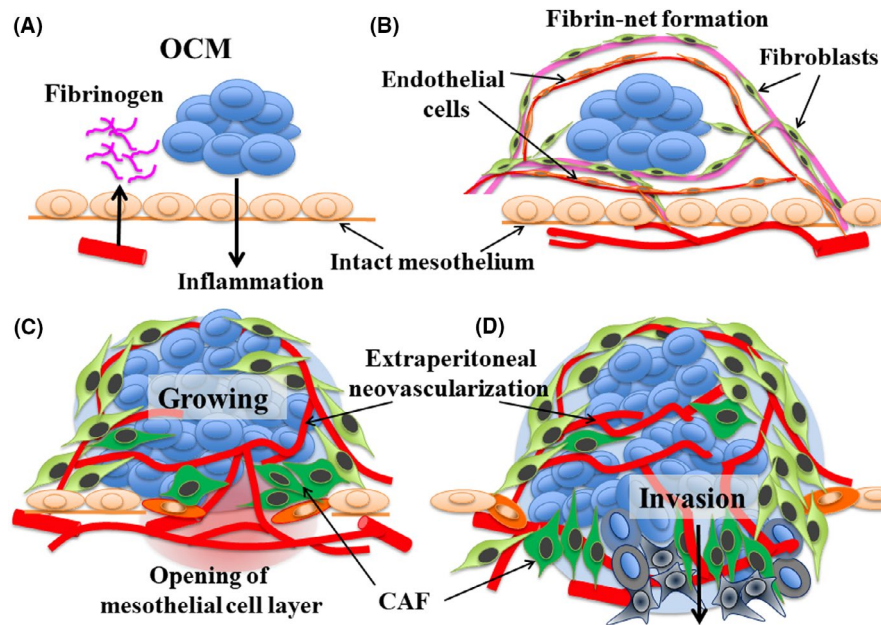


**FIGURE 5** A proposed new strategy for peritoneal implantation by ovarian cancer cells. A, Step I. Ovarian cell masses (OCMs) cause an inflammatory reaction on the peritoneal stroma, inducing the leakage of fibrinogen. B, Step II. OCM are anchored and surrounded by fine fibrin networks without adhering to the peritoneal epithelium, inducing the migration of fibroblasts and endothelial cells from the host's tissues toward the fibrin networks. C, Step III. Fibrin networks around OCM become mature stromal tissues, developing vascular networks, growing OCM, differentiating cancer-associated fibroblasts (CAF), inducing inflammation around vessel-insertion sites, and extending the opening area of the intact mesothelial cell layer. D, Step IV. The boundary layer of mesothelial cells disappears and both intraperitoneal host stromal tissues and extraperitoneal OCM-surrounding stromal tissues are integrated together, enabling the OCM to invade the host stroma, being accompanied by CAF

For the 2nd step, the fibrin-net structure traps the OCMs in peritoneal fluids, anchoring these to the peritoneal wall. As TF, which converts fibrinogen to fibrin, was clearly detected on the OCM-anchoring fibrin net (Figure 1H), the fibrous network may

be constructed from the exudated fibrinogen by TF. It should be noted that fibrin was reported to contribute to successful tumor implantation by allowing metastatic cells to provide requisite signals for adhesion to the peritoneal wall and neovascularization in the

underlying peritoneal stroma through local inflammation, promoting the production of ascites.<sup>13,14</sup> As a novel finding, this study showed that these fibrin nets can offer a framework for the subsequent migration of CD31/CD34/VEGF-A-positive endothelial cells and podoplanin-positive fibroblasts. This process may be fundamentally based on tissue remodeling and repair mechanisms through coagulation systems. Surprisingly, these endothelial cells then constructed fine functional vessel networks, which contained circulating red blood cells, around OCM outside the intact mesothelial cell layer (Figure 1M,N).

For the 3rd step, vascular networks became established around OCM. In addition, fibroblasts around OCM enhance the expression of CAF markers,  $\alpha$ SMA, and podoplanin. These stromal cells and OCM express SDF-1/CXCL12 (Figure 2F), which was reported to induce invasive activity in various cancer cells.<sup>15-18</sup> Considering that the volume of OCMs was largely greater than those in the fibrous nets, the development of the blood supply may contribute to growing and activating OCM outside the intact mesothelial cell layer. Around the insertion sites of feeding vessels, local inflammation was induced by the OCM or CAF, leading to disruption of the mesothelial cell barrier.

For the final step, the mesothelial cell layer disappeared, creating a wide area allowing direct interaction with the OCM-surrounding stroma and resident peritoneal stroma. In this stage, OCM invaded resident peritoneal stroma through the disrupted area that contained feeding vessels, being accompanied by CAF.

We hypothesized that the coagulation system is involved in the initial process of peritoneal implantation. To investigate this, immunoreactive TF was evaluated and found to be abundant in OCM (Figures 1H, 2C, 3C,I). Previous reports have suggested that cytokine-induced and/or chemokine-induced TF expression in tumor cells and tumor-connective tissues promotes neo-angiogenesis, invasion, and metastasis in ovarian cancer.<sup>3,19</sup> Recently, Matsumura's group.<sup>20-22</sup> demonstrated that the systemic administration of selective anti-TF antibody conjugated with an anti-cancer drug was effective for growth inhibition of human pancreatic and gastric cancer cell lines using murine intravenous xenograft models without affecting coagulant activity. Importantly, this effect was also observed in xenograft experiments using a TF-low-expressing cancer cell line, suggesting the metastatic tumor-induced TF expression in adjacent stromal cells.<sup>21</sup> Conversely, intraperitoneal chemotherapy has been accepted as one of the effective strategies against ovarian cancers.<sup>23</sup> Consequently, considering high TF expression in ascites and around implanting OCM on the outer side of the peritoneal wall, the intraperitoneal administration of anti-TF antibody conjugated with an anti-cancer drug may become one of the prospective therapies against ovarian cancers.

The main limitation of this report is that the proposed strategy is fundamentally based on morphological findings in only 6 patients. The lack of molecular experiments to support the expression of key factors and absence of in vitro or animal experiments to confirm the proposed strategy are also weak points. However, approximately half the total number of cases with serous carcinoma (6 in 13)

showed similar histological images of extraperitoneal growth along with the feeding vessels from noninvaded intraperitoneal stroma. This sign represents a novel cascade of peritoneal invasion by ovarian cancers. Consequently, wide recognition or evaluation of the presence of this type of peritoneal invasion by basic researchers and clinical oncologists will contribute to developing new strategies for the treatment of patients with carcinomatous peritoneal dissemination. Further analysis of other cases showing similar phenomena and additional basic experiments on the effectiveness of this strategy will be necessary in the future.

Here we report several cases of ovarian serous carcinoma showing unique processes of peritoneal invasion. From morphological and immunohistochemical findings, we propose a new strategy of peritoneal implantation by ovarian cancer cells, which is initiated by neovascularization around fibrin-anchored OCM on the outer side of the intact peritoneal surface. This discovery may lead to a paradigm shift in the concept of peritoneal implantation of cancer. Further clarification of the mechanisms of these cascades will contribute to developing new therapeutic approaches against ovarian cancers, concomitantly providing valuable information on peritoneal implantation of other cancers.

## ACKNOWLEDGMENTS

The authors are grateful to Professor Kyo at Shimane University, Professor Mikami at Kumamoto University, and Professor Matsumura at Kinki University for valuable discussion regarding the manuscript. This work was supported in part by Grants-in-Aid for Scientific Research (grant nos. 17H04337 and 18K16762).

## DISCLOSURE

The authors declare that they have no conflict of interest.

## ORCID

Yasunari Mizumoto  <https://orcid.org/0000-0001-8648-3696>

## REFERENCES

1. Partridge EE, Barnes MN. Epithelial ovarian cancer: prevention, diagnosis, and treatment. *CA Cancer J Clin.* 1999;49:297-320.
2. Ozols RF, Bookman MA, Connolly DC, et al. Focus on epithelial ovarian cancer. *Cancer Cell.* 2004;5:19-24.
3. Wang X, Wang E, Kavanagh JJ, Freedman RS. Ovarian cancer, the coagulation pathway, and inflammation. *J Transl Med.* 2005;3:25.
4. Shield K, Ackland ML, Ahmed N, Rice GE. Multicellular spheroids in ovarian cancer metastasis: biology and pathology. *Gynecol Oncol.* 2009;113:8143-8148.
5. Matte I, Legault CM, Garde-Granger P, et al. Mesothelial cells interact with tumor cells for the formation of ovarian cancer multicellular spheroids in peritoneal effusions. *Clin Exp Metastasis.* 2006;33:829-852.
6. Yin M, Li X, Tan S, et al. Tumor-associated macrophages drive spheroid formation during early transcoelomic metastasis of ovarian cancer. *J Clin Invest.* 2016;126:4157-4173.



7. Masoumi Moghaddam S, Amini A, Morris DL, Pourgholami MH. Significance of vascular endothelial growth factor in growth and peritoneal dissemination of ovarian cancer. *Cancer Metastasis Rev.* 2012;31:143-162.
8. Ahmed N, Thompson EW, Quinn MA. Epithelial-mesenchymal inter-conversions in normal ovarian surface epithelium and ovarian carcinomas: an exception to the norm. *J Cell Physiol.* 2007;213:581-588.
9. Auer K, Bachmayr-Heyda A, Aust S, et al. Peritoneal tumor spread in serous ovarian cancer-epithelial mesenchymal status and outcome. *Oncotarget.* 2015;6:17261-17275.
10. Thiery JP, Acloque H, Huang RY, Nieto MA. Epithelial-mesenchymal transitions in development and disease. *Cell.* 2009;139:871-890.
11. Obata T, Nakamura M, Mizumoto Y, et al. Dual expression of immunoreactive estrogen receptor  $\beta$  and p53 is a potential predictor of regional lymph node metastasis and postoperative recurrence in endometrial endometrioid carcinoma. *PLoS ONE.* 2017;12(11):e0188641.
12. Malarstig A, Tenno T, Jossan S, Aberg M, Siegbahn A. A quantitative real-time PCR method for tissue factor mRNA. *Thromb Res.* 2003;112:175-183.
13. Nagy JA, Meyers MS, Masse EM, et al. Pathogenesis of ascites tumor growth: fibrinogen influx and fibrin accumulation in tissues lining the peritoneal cavity. *Cancer Res.* 1995;55:369-375.
14. Nagy JA, Morgan ES, Herzberg KT, et al. Pathogenesis of ascites tumor growth: angiogenesis, vascular remodeling, and stroma formation in the peritoneal lining. *Cancer Res.* 1995;55:376-385.
15. Kim YH, Choi YW, Lee J, et al. Senescent tumor cells lead the collective invasion in thyroid cancer. *Nat Commun.* 2017;8:15208.
16. Guo F, Wang Y, Liu J, et al. CXCL12/CXCR16: a symbiotic bridge linking cancer cells and their stromal neighbors in oncogenic communication networks. *Oncogene.* 2016;35:816-826.
17. Sorrentino C, Miele L, Porta A, et al. Activation of the A2B adenosine receptor in B16 melanomas induces CXCL12 expression in FAP-positive tumor stromal cells, enhancing tumor progression. *Oncotarget.* 2016;7:64274-64288.
18. Orimo A, Gupta PB, Sgroi DC, et al. Stromal fibroblasts present in invasive human breast carcinomas promote tumor growth and angiogenesis through elevated SDF-1/CXCL12 secretion. *Cell.* 2005;121:335-348.
19. Belting M, Dorrell MI, Sandgren S, et al. Regulation of angiogenesis by tissue factor cytoplasmic domain signaling. *Nat Med.* 2004;10:502-509.
20. Yamamoto Y, Hyodo I, Koga Y, et al. Enhanced antitumor effect of anti-tissue factor antibody-conjugated epirubicin-incorporating micelles in xenograft models. *Cancer Sci.* 2015;106:627-634.
21. Koga Y, Manabe S, Aihara Y, et al. Antitumor effect of antitissue factor antibody-MMAE conjugate in human pancreatic tumor xenografts. *Int J Cancer.* 2015;137:1457-1466.
22. Sugaya A, Hyodo I, Koga Y, et al. Utility of epirubicin-incorporating micelles tagged with anti-tissue factor antibody clone with no anticoagulant effect. *Cancer Sci.* 2016;107:335-340.
23. Karam A, Ledermann JA, Kim JW, et al. Participants of the 5th Ovarian Cancer Consensus Conference. Fifth ovarian cancer consensus conference of the gynecologic cancer intergroup: first-line interventions. *Ann Oncol.* 2017;28:711-717.

**How to cite this article:** Matsuoka A, Mizumoto Y, Ono M, et al. Novel strategy of ovarian cancer implantation: Pre-invasive growth of fibrin-anchored cells with neovascularization. *Cancer Sci.* 2019;110:2658-2666. <https://doi.org/10.1111/cas.14098>